J. FAC. SCI., SHINSHU UNIVERSITY, Vol. 38, pp.23-34 2003

Variations of divalent cation concentrations in pore water and the precipitation of Mg-rich authigenic mineral during early diagenesis of Toyoma Formation

Toshiro MORIKIYO*, Kinuko MATSUNAGA*, Kazuo IWAMASA* and Satoshi KANISAWA**

*Department of Geology, Faculty of Science, Shinshu University, Asahi 3-1-1, Matsumoto 390-8621, Japan

**2-19-14, Yagiyama-Honcho, Taihaku-ku, Sendai 982-0801, Japan

(Received October 15, 2003)

Abstract

The variations of Fe, Mn and Mg concentrations in pore water were deduced from the chemistry of calcite. With depth, the Fe/Ca, Mn/Ca, Mg/Ca ratios of pore water decrease. The decrease in the Fe/Ca ratio is due to the precipitation of pyrite, whereas the decrease in the Mn/Ca ratio is due to the precipitation of Mn-rich calcite. The depletion of Mg in pore water is ascribed to the precipitation of either Mg-rich smectite or Mg-rich chlorite. A-type rock is further divided into A1 and A2 subtypes, on the basis of $\delta^{13}C$. Excesses of MgO and deficiencies of K_2O above the calculated whole-rock compositions are observed mainly in the phosphatic nodules and A1 subtype. This suggests that the formation of Mg-rich smectite or Mg-rich chlorite took place at very early stage of diagenesis of the Toyoma Formation.

Introduction

The variation of the supersaturation rate of pore water with respect to the pyrite, apatite and calcite components was obtained in the preceding paper (Morikiyo and Matsunaga, 2001 ; Matsunaga, 2000). However, the variation of the cation concentrations of pore water with the progress of diagenesis was not dealt in that paper. The following exchange reactions take place between calcite and pore water at the time of calcite precipitation :

$(Ca^{2+}CO_3)$calcite + (M^{2+})pore water = $(M^{2+}CO_3)$calcite + (Ca^{2+})pore water.

Here M^{2+} represents such divalent cations as Mg^{2+}, Fe^{2+} and Mn^{2+}. For the above reactions, $Kd=(\mathbf{a}_M/\mathbf{a}_{Ca})$calcite/$(\mathbf{a}_M/\mathbf{a}_{Ca})$pore water, where **a** is the activity for the elements and Kd is the equilibrium constant for the exchange reaction. Thus, (M^{2+}/Ca)calcite is equal to $Kd\times(M^{2+}/Ca)$pore water. From this relationship, we can consider

(M^{2+}/Ca) ratio of calcite to be proportional to (M^{2+}/Ca) ratio of pore water.

In this paper, the variation of divalent cation concentrations of pore water is

Table 1 Chemical composition of the acid-soluble fraction of phosphatic and carbonate rocks in the Toyoma Formation.

CO_2 (%) is reproduced from Kanisawa and Ehiro (1986). FeO, MnO, MgO and CaO concentrations were those of acid (1/10N acetic acid)-soluble fractions. The CO_2calc.(%) values were obtained from the concentrations, assuming the stoichiometry of calcite. X values are atomic proportions of divalent cations in calcite, i.e., $X_{Fe}=100\times Fe/(Fe+Mn+Mg+Ca)$. Atomic ratio of Fe to Ca for the acid-soluble fraction is shown as Fe/Ca.

Specimen Number	CO_2 (%)	FeO (%)	MnO (%)	MgO (%)	CaO (%)	CO_2calc. (%)	X_{Fe}	X_{Mn}	X_{Mg}	X_{Ca}	Fe/Ca	Mn/Ca	Mg/Ca
Phosphatic nodules													
P-20	8.13	0.20	0.31	0.08	9.73	8.04	1.52	2.39	1.09	95.00	0.016	0.025	0.011
UP-29(3)	4.18	0.05	0.14	0.18	4.52	3.86	0.79	2.25	5.09	91.87	0.009	0.024	0.055
UP-29(1)	8.22	0.23	0.38	0.17	9.93	8.36	1.69	2.82	2.22	93.27	0.018	0.030	0.024
KI01-4		0.52	2.23	0.20	12.92	12.06	2.64	11.47	1.81	84.08	0.031	0.136	0.022
KI01-2		0.56	2.37	0.22	14.04	13.07	2.62	11.25	1.84	84.29	0.031	0.133	0.022
U-N171		0.43	1.89	0.23	12.83	11.76	2.24	9.97	2.14	85.65	0.026	0.116	0.025
UP-59A	1.15	0.07	0.11	0.25	1.82	1.81	2.37	3.77	15.06	78.81	0.030	0.048	0.191
UP-59C	0.69	0.07	0.10	0.23	1.63	1.64	2.62	3.79	15.36	78.23	0.034	0.048	0.196
OP-1	0.59	0.01	0.00	0.15	0.40	0.48	1.27	0.00	33.85	64.88	0.020	0.000	0.522
UP-17	0.12	0.01	0.00	0.12	0.42	0.47	1.31	0.00	28.07	70.62	0.019	0.000	0.397
A type													
U-A03		0.14	0.17	0.22	11.80	9.69	0.88	1.09	2.48	95.55	0.010	0.012	0.028
UP-32	2.72	0.12	0.20	0.22	1.42	1.55	4.74	7.99	15.47	71.80	0.066	0.111	0.216
U-A01		0.63	0.17	0.28	8.81	7.71	5.00	1.37	3.96	89.66	0.056	0.015	0.044
OP-6	12.78	0.23	0.51	0.18	15.22	12.60	1.11	2.51	1.56	94.81	0.012	0.026	0.016
UP-4	20.79	0.26	0.69	0.22	24.34	19.93	0.80	2.15	1.21	95.85	0.008	0.022	0.013
UP-11	26.10	0.39	0.78	0.13	30.40	24.72	0.97	1.96	0.57	96.50	0.010	0.020	0.006
UP-43	19.29	0.10	0.44	0.16	18.61	15.11	0.41	1.81	1.16	96.63	0.004	0.019	0.012
U-A11		0.29	0.35	0.13	5.84	5.12	3.47	4.24	2.77	89.52	0.039	0.047	0.031
OP-3	11.15	0.12	0.68	0.08	13.06	10.83	0.68	3.89	0.81	94.62	0.007	0.041	0.009
KI02-3a	12.58	0.25	0.30	0.12	10.02	8.33	1.84	2.23	1.57	94.36	0.019	0.024	0.017
U-A07		0.26	0.01	0.17	1.21	1.30	12.24	0.48	14.27	73.01	0.168	0.007	0.195
B type													
U-B01		0.67	0.46	0.30	13.07	11.28	3.64	2.53	2.90	90.93	0.040	0.028	0.032
UP-48	13.35	0.15	0.38	0.15	16.81	13.68	0.67	1.72	1.20	96.41	0.007	0.018	0.012
U-SS10		1.27	0.41	0.58	8.82	8.59	9.06	2.96	7.37	80.60	0.112	0.037	0.091
UP-45	16.03	0.05	0.24	0.08	18.75	14.98	0.20	0.99	0.58	98.22	0.002	0.010	0.006
UP-42U	12.66	0.09	0.30	0.10	15.51	12.52	0.44	1.49	0.87	97.20	0.005	0.015	0.009
UP-4	11.02	0.18	0.33	0.12	12.07	9.92	1.11	2.06	1.32	95.50	0.012	0.022	0.014
U-SS04		0.19	0.26	0.06	12.77	10.36	1.12	1.56	0.63	96.69	0.012	0.016	0.007
U-B04		0.42	0.57	0.12	20.10	16.52	1.56	2.14	0.79	95.51	0.016	0.022	0.008
UP-7	20.64	0.23	0.79	0.08	25.91	21.05	0.67	2.33	0.41	96.59	0.007	0.024	0.004
U-SS14		0.54	0.25	0.17	12.41	10.41	3.18	1.49	1.78	93.55	0.034	0.016	0.019
U-B07		0.96	0.30	0.34	18.80	15.90	3.70	1.17	2.33	92.80	0.040	0.013	0.025
U-B09		0.80	0.23	0.34	5.54	5.35	9.15	2.67	6.94	81.24	0.113	0.033	0.085
Pyritiferous concretions													
U-N011bul		1.95	0.40	0.20	5.49	5.97	20.01	4.16	3.66	72.18	0.277	0.058	0.051
C type													
U-C10		0.46	0.94	0.07	38.11	30.85	0.91	1.89	0.25	96.95	0.009	0.019	0.003
UP-56	37.46	0.48	1.37	0.21	43.08	35.18	0.84	2.42	0.65	96.10	0.009	0.025	0.007
UP-50	37.79	0.38	1.31	0.17	45.61	37.02	0.63	2.20	0.50	96.68	0.007	0.023	0.005
UP-7	32.66	0.36	1.34	0.15	39.42	32.15	0.69	2.59	0.51	96.22	0.007	0.027	0.005
U-C08		0.51	1.17	0.24	38.08	31.18	1.00	2.33	0.84	95.83	0.010	0.024	0.009
UP-59(1)	36.95	0.41	1.52	0.18	43.55	35.57	0.71	2.65	0.55	96.09	0.007	0.028	0.006
U-C02		0.82	0.69	0.39	35.15	28.94	1.74	1.48	1.47	95.31	0.018	0.016	0.015
UP-4	35.10	0.55	0.74	0.23	37.11	30.17	1.12	1.52	0.83	96.53	0.012	0.016	0.009
UP-10	27.41	0.38	0.98	0.20	30.41	24.92	0.93	2.44	0.88	95.75	0.010	0.025	0.009
U-C11		0.57	1.14	0.20	42.44	34.58	1.01	2.05	0.63	96.31	0.010	0.021	0.007
UP-63	38.35	0.55	1.03	0.22	40.47	32.98	1.02	1.94	0.73	96.31	0.011	0.020	0.008
UP-35	29.63	0.65	0.63	0.23	33.68	27.47	1.45	1.42	0.91	96.21	0.015	0.015	0.010

estimated from the chemistry of a calcite solid solution. Then the causes for the variations are investigated.

Analytical methods

The chemical analyses of CaO, MnO, FeO and MgO in acid-soluble (1/10N acetic acid) fractions of the rocks were carried out by the atomic absorption method. The analytical procedure follows that described by Kanisawa and Ehiro (1986).

Results

The results of chemical analyses for acid-soluble components are shown in Table 1. The CO_2 percent by weight was calculated from the concentrations of CaO, MgO, FeO and MnO in the samples using the assumption that divalent cations were derived only from carbonate mineral. The calculated CO_2 percentages are cited as CO_2calc.%. Kanisawa and Ehiro (1986) have shown that CO_2calc.% agrees well with the CO_2 content determined analytically. Thus, it is reasonable to say that the divalent cation composition of the acid solution represents the chemical composition of calcite contained in the phosphatic and carbonate rocks.

Here, the atomic ratio $100 \times Ca/(Fe+Mg+Mn+Ca)$ is designated as X_{Ca}. Fig. 1

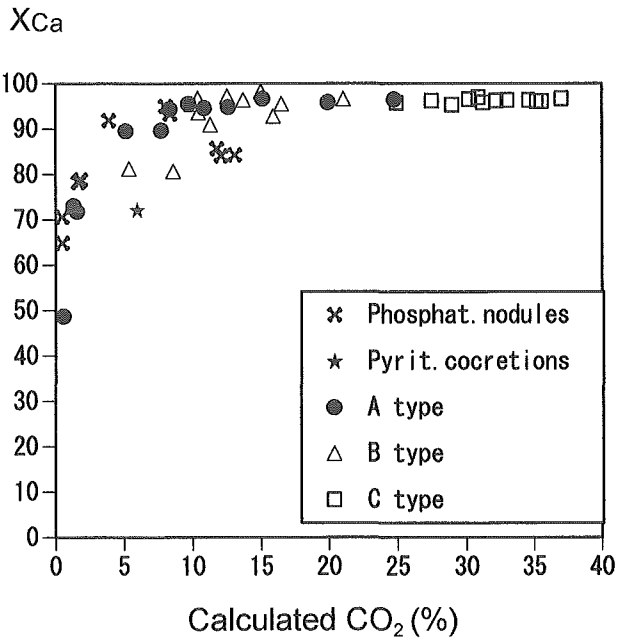

Fig. 1 Plot of X_{Ca} ($=100 \times Ca/(Fe+Mn+Mg+Ca)$ against calculated CO_2 content (CO_2calc. (%)) for all rock samples.

shows the relationship between X_{Ca} and CO_2calc.%. Calcite in the phosphatic nodules and the A-type rock with a low-CO_2 content shows a lower X_{Ca} value, indicating that the calcite in those rocks is impure. The X_{Ca} of A-type rock increases with the value of CO_2calc.%. Calcite from C-type rock has an X_{Ca} value around 96. It is clear from Fig. 1 that the chemistry of a calcite solid solution varies with the increase of whole-rock carbonate content in the rocks, which is also a measure of the progress of diagenesis.

Fig. 2 shows the relationship between the Fe/Ca, Mn/Ca, Mg/Ca ratios and CO_2 calc.% for the rocks. The Fe/Ca ratios for the A- and B-type rocks are high in the samples having low CO_2calc.%, and the ratio decreases with an increase of CO_2calc.%. C-type rock shows very low and constant Fe/Ca ratios. As a whole, the ratio decreases with increased CO_2 content. The Mn/Ca ratio for A-type rock is very high in portions where CO_2calc.% is lower than 2%. Then it decreases steeply with an increase of CO_2 content but it does not reach 0. The Mn/Ca ratio for the rocks of higher CO_2 is about 0.02, and is nearly uniform. The Mn/Ca ratios of three phosphatic nodules lie outside of the trend. The Mg/Ca ratio is very high where CO_2 content is lower than 2%. The ratio decreases steeply with the rise in CO_2 content. The Mg/Ca ratio is close to 0 at the point where CO_2calc.% is about 10%. Compared with the other two ratios, the Mg/Ca ratio represents a smooth trend.

Discussion

Variations of divalent cation concentrations in pore water

Kanisawa and Ehiro (1986) confirmed that divalent cations in the 1/10 N acetic acid-soluble fraction were derived from carbonate mineral contained in the rocks. However, the possibility that metal ions, which are absorbed into mica-clay mineral surfaces dissolved in an acid solution, if the carbonate content is low, cannot be ruled out (Kitano, 1990). As the results show, the proportions of Fe, Mg and Mn ions among the four ions (Fe, Mn, Mg and Ca) in the acid-soluble fractions are notably high for the phosphatic nodules and A-type rock, in which the carbonate content is remarkably low. Thus, we examined the effect of contamination of those ions from mica-clay minerals and hydroxides.

The positive correlation between MgO+FeO wt.% and CaO wt.% in the phosphatic nodules is shown in Fig. 3. Since Ca ion is accommodated only in calcite, the existence of a positive correlation indicates that the Fe and Mg ions were also derived from carbonate minerals. Therefore, we may safely conclude that divalent cations in the acid-soluble fraction were derived from carbonate minerals even for rocks with a low carbonate content.

As noted before (Morikiyo and Matsunaga, 2001; Matsunaga, 2000), the CO_2 content of the rocks can be used as a measure for the progress of diagenesis. The Fe/

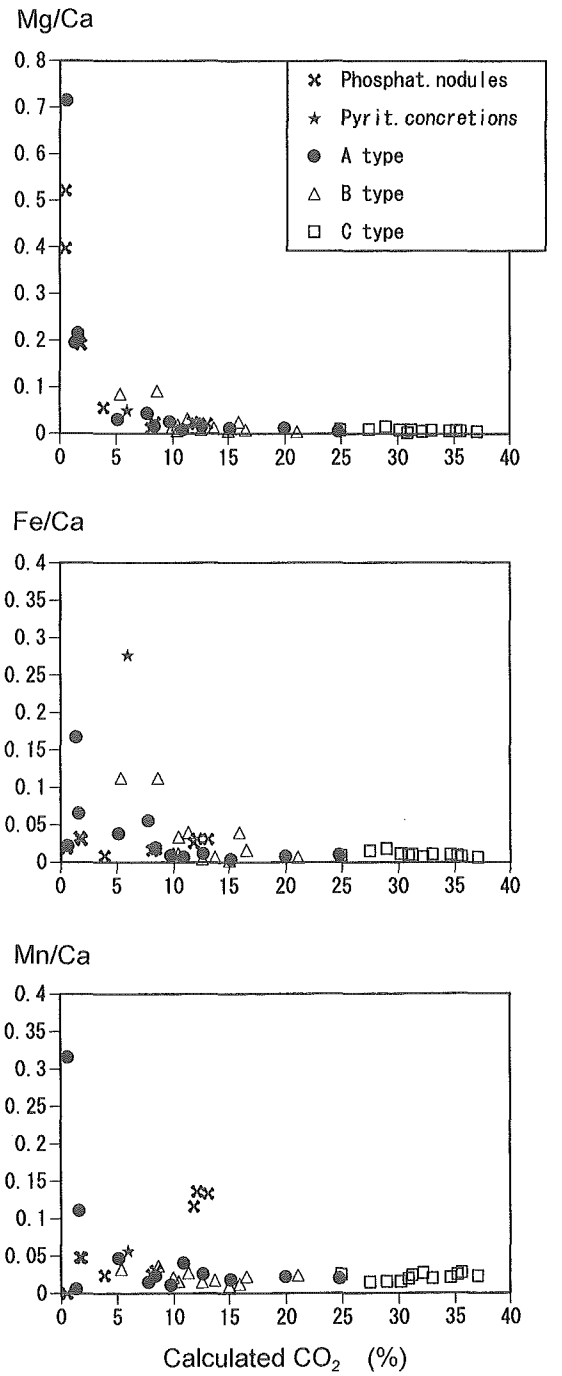

Fig. 2 Plot of the M^{2+}/Ca ratio of acid-soluble component against calculated CO_2 content. The top: Mg/Ca ratio, the middle: Fe/Ca ratio, the bottom: Mn/Ca ratio.

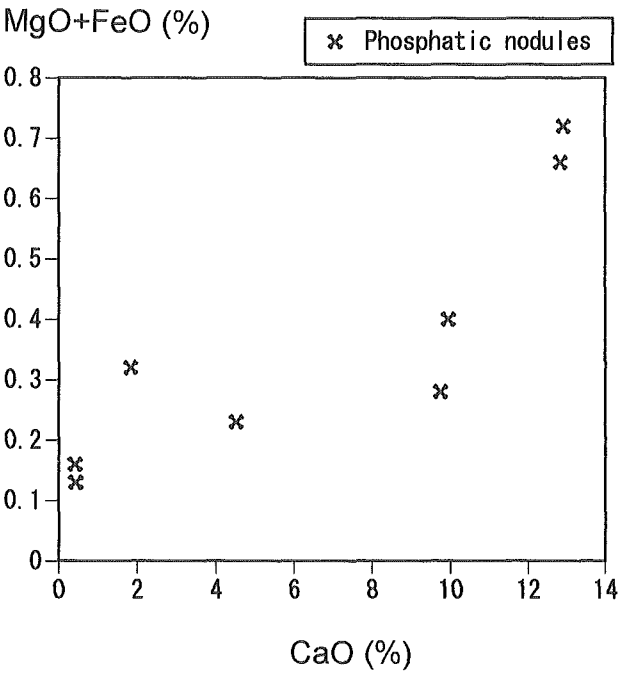

Fig. 3 Plot of the sum of MgO and FeO content (wt. %) against CaO content (wt. %) for the phosphatic nodules.

Ca, Mn/Ca, Mg/Ca ratios of calcite reflect the presence of these ratios in pore water. Thus, Fig. 1 and 2 represent the chemical change of pore water with the progress of diagenesis. In these diagrams, the abscissa represents CO_2calc.%, which is calculated from Fe, Mn, Mg and Ca concentrations of the acid-soluble fractions, assuming a stoichiometry of carbonate. The $\delta^{13}C$ values for the samples can be estimated from whole-rock CO_2 % (either measured or calculated) by using the equation:

$\delta^{13}C(‰) = -0.238 \times CO_2wt\% - 6.31$

which was obtained in the preceding paper (Morikiyo and Matsunaga, 2001).

Fe Fe/Ca ratios of calcite are scattered in samples with low CO_2 content (Fig. 2, the middle). However, this ratio decreases with an increase in CO_2 content and comes close to 0 at CO_2calc.%=20. Such a CO_2 content correspond to a $\delta^{13}C$ value of $-11‰$. It should be noted that the proportion of normative pyrite among the three normative minerals (X'_{Pyrite}) also becomes nearly 0 at $\delta^{13}C = -11.5‰$ (Morikiyo and Matsunaga, 2001). Thus, we conclude that decreases in the Fe/Ca ratio of pore water with increases in sediment burial are due to the precipitation of pyrite.

Mn The Mn/Ca ratio is greatest at the shallowest burial depths (CO_2calc.%=0 −2), then suddenly decreases with an increase in CO_2calc.%(Fig. 2, the bottom). At

depths where CO_2 content is greater than 7.5%, the Mn/Ca ratio of calcite has a constant value of about 0.02. This may indicate that the reduction of manganese oxide persisted to a greater sediment depth. The early depletion of Mn ion in pore water may be due to the precipitation of Mn-rich calcite, because it has been ascertained that all the MnO present in a rock is accommodated in the calcite (Kanisawa and Ehiro, 1986).

Mg The Mg/Ca ratio of pore water is high at shallow burial depths (Fig. 2, the top), which is natural because pore water originated as seawater. With deeper sediment burial, the Mg/Ca ratio conspicuously decreases and becomes nearly 0 at CO_2 calc.%=10. This indicates that Mg ions were eliminated from the pore water through formation of a certain Mg-rich mineral during early diagenesis. Calcite is not a candidate for this mineral, because the amount of calcite precipitated during that stage is very small and, in addition, the $MgCO_3$ component of the calcite is also small. The crystallization of trioctahedral Mg-rich smectite (saponite) or Mg-rich chlorite must be responsible for the depletion of Mg ions in pore water. This point will be further discussed in the next chapter.

Precipitation of Mg-rich mineral in very early stage of diagenesis

The normative content of pyrite, apatite, calcite and black shale were obtained as previously described (Morikiyo and Matsunaga, 2001; Matsunaga, 2000). From the chemistries of the normative minerals and their proportions in a given rock sample, the whole-rock MgO, Na_2O and K_2O content was calculated and is shown in Table 2 and

Table 2 Measured and calculated whole-rock chemical compositions of phosphatic and carbonate rocks from the Toyoma Formation.
Chemical compositions of the samples are from Kanisawa and Ehiro (1986). The weight percent of oxides calculated from the norm composition and ideal chemical composition of the minerals is designated as MgOcalc., etc. The norm compositions as well as the procedures for the calculation have been described in Matsunaga (2000). The $\delta^{13}C$ (‰) values in parentheses are those estimated from the whole-rock CO_2 content. Abbreviations for rock type: N: Phosphatic nodules; A: A-type rock.

Rock type	N	N	N	A	A	A	A	A	A	A	A
Specimen Number	UP-59A	UP-29 (3)	OP-1	UP-11	OP-2	OP-4	OP-3	UP-4	OP-5	UP-32	UP-20
MgO	2.39	2.53	3.97	0.75	1.89	2.71	1.84	1.16	2.31	3.31	2.95
CaO	24.87	23.59	7.17	41.29	31.50	29.54	30.64	32.13	24.29	8.21	11.44
Na_2O	1.14	0.29	0.67	0.66	0.56	0.22	0.65	1.32	0.40	0.49	0.40
K_2O	0.71	0.06	0.67	0.56	0.79	0.31	0.58	0.77	0.26	0.81	0.21
Calculated											
MgOcalc.	1.25	1.37	2.11	1.05	1.28	1.22	1.15	1.42	1.53	1.47	2.18
CaOcalc.	25.56	23.57	8.44	38.96	27.77	27.99	30.48	30.13	22.37	10.32	13.06
Na_2Ocalc.	0.90	0.95	1.54	0.42	0.65	0.67	0.69	0.76	1.01	1.04	1.50
K_2Ocalc.	1.44	1.53	2.47	0.68	1.05	1.07	1.11	1.22	1.63	1.67	2.41
$\delta^{13}C$(‰)	(-6.6)	-7.2	(-6.5)	-10.5	(-11.3)	-9.0	-11.4	-9.9	(-8.2)	-7.1	(-8.0)

Table 3 Measured and calculated whole-rock chemical compositions of phosphatic and carbonate rocks from the Toyoma Formation.
Partial chemical analyses are from Kanisawa and Ehiro (1986). The weight percent of oxides calculated from the norm composition and ideal chemical composition of the minerals is designated as MgOcalc., etc. The norm compositions as well as the procedures for the calculation have been described in Matsunaga (2000). The $\delta^{13}C$ (‰) values in parentheses are those estimated from the whole-rock CO_2 content. Abbreviations for rock type: N: Phosphatic nodules; A: A-type rock; C: C-type rock.

Rock type	N	N	N	N	A	A	A	A	A	A
Specimen Number	UP-59C	UP-29 (1)	UP-17	P-20	UP-43	OP-6	UP-59U (2)	UP-7	UP-1	UP-10
MgO	3.59	1.97	2.86	3.34	1.69	2.52	2.58	1.79	1.12	1.03
CaO	15.63	23.59	8.84	10.25	35.23	24.97	23.37	19.59	37.37	35.38
Na_2O	1.08	0.38	0.39	0.51	1.34	0.34	1.47	0.74	1.11	0.90
K_2O	0.66	0.29	0.13	0.24	0.63	0.56	0.48	0.66	0.64	0.57
Calculated										
MgOcalc.	1.50	1.41	1.73	1.73	1.19	1.31	1.41	1.42	1.16	1.16
CaOcalc.	16.68	21.93	10.45	11.44	33.86	25.04	23.97	24.02	36.54	35.72
Na_2Ocalc.	1.09	0.92	1.27	1.16	0.61	0.79	0.87	0.86	0.52	0.53
K_2Ocalc.	1.74	1.48	2.03	1.86	0.98	1.27	1.39	1.38	0.84	0.85
$\delta^{13}C$(‰)	(-6.5)	-7.9	(-6.3)	-6.8	-10.5	-9.2	(-9.2)	(-9.6)	(-12.1)	(-12.1)

Rock type	A	A	A	A	A	A	A	A
Specimen Number	UP-57	UP-49	UP-53	UP-55	UP-46	UP-17	UP-42L	UP-41
MgO	1.29	1.40	1.27	1.59	1.02	2.01	2.08	2.31
CaO	27.52	25.13	36.35	25.86	35.46	26.73	16.39	14.74
Na_2O	1.45	1.06	0.98	1.37	0.93	0.26	2.63	2.33
K_2O	1.09	1.66	0.73	1.30	1.09	0.15	1.28	1.99
Calculated								
MgOcalc.	1.53	1.60	1.19	1.56	1.38	1.25	1.92	2.05
CaOcalc.	27.40	25.79	36.42	26.50	34.43	26.73	16.83	13.91
Na_2Ocalc.	0.87	0.93	0.5	0.89	0.65	0.64	1.24	1.36
K_2Ocalc.	1.40	1.49	0.81	1.42	1.04	1.02	1.99	2.19
$\delta^{13}C$(‰)	(-10.7)	(-10.6)	(-12.9)	(-10.9)	-16	(-11.3)	(-9.3)	(-8.7)

Rock type	C	C	C	C	C	C	C	C	C	C
Specimen Number	UP-10	UP-35	UP-59	UP-7	UP-4	UP-50	UP-63	UP-56	UP-20	UP-59 (1)
MgO	0.93	0.74	0.96	0.59	0.54	0.35	0.47	0.51	0.61	0.55
CaO	34.30	38.21	36.54	40.55	47.53	48.34	48.72	46.61	48.53	45.44
Na_2O	1.01	0.97	0.98	0.59	0.64	0.46	0.34	0.56	0.42	0.64
K_2O	1.22	0.99	1.01	0.91	0.54	0.36	0.35	0.48	0.55	0.43
Calculated										
MgOcalc.	1.40	1.32	1.36	1.24	1.09	1.04	1.02	1.04	1.03	1.06
CaOcalc.	33.69	36.23	35.42	39.66	42.53	45.67	46.32	45.23	45.71	44.65
Na_2Ocalc.	0.66	0.57	0.61	0.47	0.33	0.25	0.23	0.26	0.25	0.28
K_2Ocalc.	1.05	0.92	0.98	0.75	0.53	0.41	0.37	0.42	0.39	0.45
$\delta^{13}C$(‰)	-13.7	-15.0	(-13.2)	-12.0	-12.8	-11.6	-14.7	-11.4	(-15.3)	-12.1

3. It is clear that the calculated MgO, Na_2O, and K_2O content of the phosphatic nodules and A-type rock (especially the samples with higher $\delta^{13}C$ values) does not agree well with those obtained by chemical analysis. The relationships between the calculated and measured content of MgO, Na_2O and K_2O for the rocks are shown in Fig. 4. Here, A-type rock is divided into two subtypes, A1 and A2. The A1-type has $\delta^{13}C$ values higher than $-10‰$, and the A2-type has values lower than $-10‰$. The measured MgO content of the phosphatic nodules and A1-type rock is always higher than the calculated MgO content. On the other hand, the measured K_2O content of the rocks is always lower than the calculated content. Deviation from the 1 : 1 line is strongest for the phosphatic nodules, followed by the A1-type rock. The A2-type rock plots around the 1 : 1 line. Data points for Na_2O as a whole show a similar, if not conspicuous, tendency as those for K_2O.

There is a possibility that the deviation from the 1 : 1 line arose from the inappropriate composition of shale used for the rock norm calculation. If we use the composition of unusual shale for the norm calculation, whose MgO/SiO_2 ratio is lower than that of the representative shale of the Toyoma Formation, then the measured MgO content must become higher than the calculated MgO content. This is because the amount of "normative shale component" is calculated from the SiO_2 content of a sample (Morikiyo and Matsunaga, 2001, Matsunaga, 2000).

In order to examine the possibility above, the frequency distribution for MgO, K_2O and Na_2O contents of the black shale from the Toyoma Formation is shown as histograms (Fig. 5). The concentrations used for the norm calculations (the average composition of JSL-1 and JSL-2) plot almost in the center of the ranges for MgO, K_2O and Na_2O contents. Thus using the average composition of JSL-1 and JSL-2 for the calculation is justified. Therefore, the deviation from the 1 : 1 line observed for MgO, K_2O and Na_2O concentrations of the phosphatic nodules and A1-type rock are not artifacts. These lines of evidence strongly suggest that a certain Mg-rich mineral, which is present in much higher amounts than in the black shale, is present in the phosphatic nodules and A1-type rock.

The Mg-rich mineral is considered to be either Mg-rich smectite or Mg-rich chlorite. Trioctahedral ferromagnesian smectites were found to be the predominant authigenic clay minerals in Recent submarine sediments (Güven, 1988). Chlorite is commonly found in Recent deep-sea clay in the Atlantic and other oceans (Biscaye, 1965). Most of the chlorite occurring in marine sediments, however, has been regarded to be detrital in origin (Griffin et al., 1968 ; Open University Course Team, 1989). But, the occurrence of authigenic chlorite from gibbsite in ocean bottom sediments has been also reported (Swindale and Fan, 1967). From the data obtained in this study, we cannot conclude which mineral, Mg-rich smectite or Mg-rich chlorite, was formed at the very early stage of diagenesis of the Toyoma Formation. Although chlorite occurs

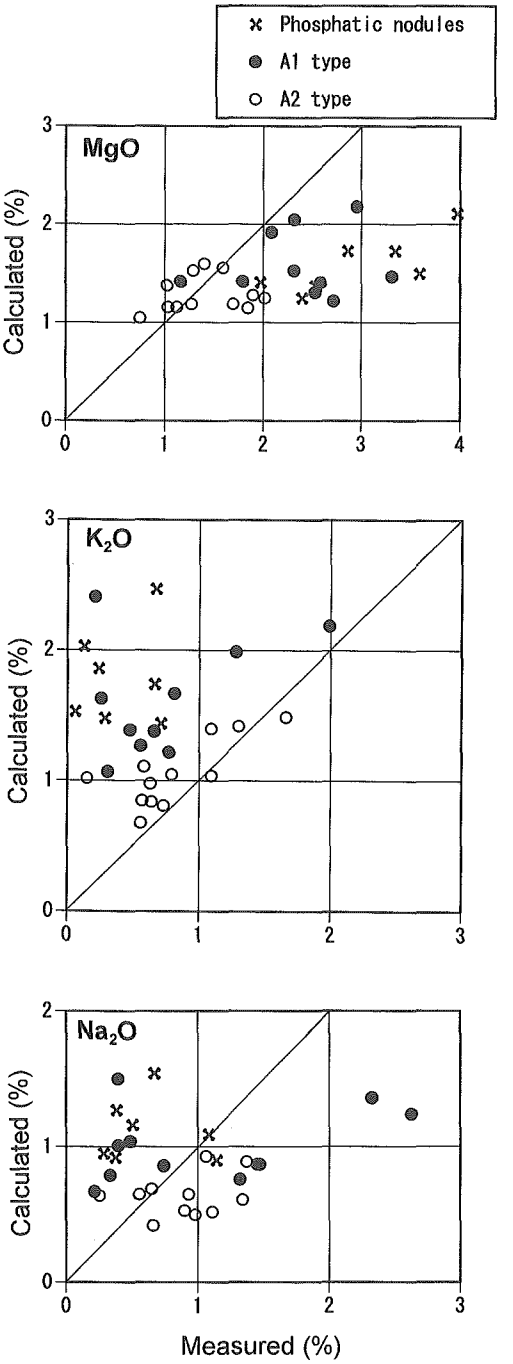

Fig. 4 Plot of calculated oxide content versus measured oxide content for phosphatic nodules and A-type rock. The top : for MgO, the middle : for K_2O, the bottom : for Na_2O. A-type rock is subdivided into A1 and A2 types. The A1 type has a $\delta^{13}C$ value higher than $-10‰$ while the A2 type has a value lower than $-10‰$.

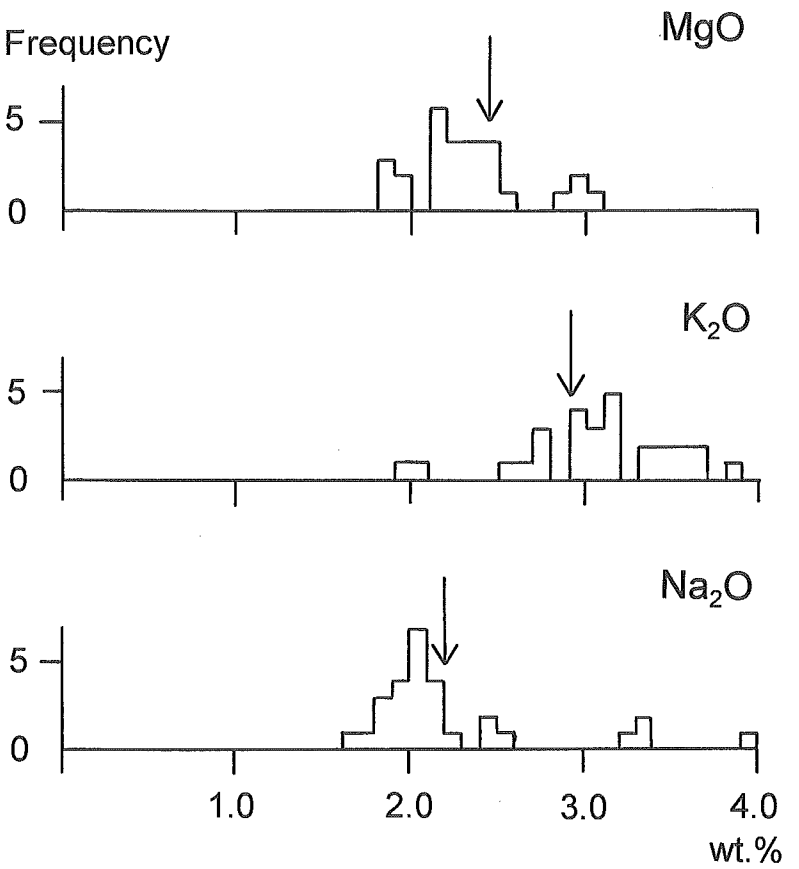

Fig. 5 Frequency distribution diagrams of MgO, K_2O, and Na_2O contents for the black shale of the Toyoma Formation.
The average composition of JSL-1 and JSL-2 for each oxide component is indicated by an arrow.

abundantly in the black shale of Toyoma Formation (Hirowatari and Katayama, 1973), its genetic process remains unsolved.

Conclusions

The variations of divalent cation concentrations of pore water were estimated from the chemistry of a calcite solid solution. Pore water became depleted in Fe^{2+}, Mn^{2+} and Mg^{2+} ions owing to the precipitation of authigenic minerals such as pyrite, Mn-rich calcite, and either Mg-rich smectite or Mg-rich chlorite as sediment burial progressed. The formation of the Mg-rich mineral in very eary stage of diagenesis is also indicated from the whole-rock chemical compositions.

Acknowledgements

The authors are grateful to Prof. M. Ehiro of Tohoku University for his help in the early stage of this work.

References

Biscaye, P.B. (1965) Mineralogy and sedimentation of Recent deep-sea clay in the Atlantic Ocean and adjacent seas and oceans. Geological Society of America Bulletin, 76, 803-832.

Griffin, J.J., Windom, H. and Goldberg, E.D. (1968) The distribution of clay minerals in the world ocean. Deep Sea Research, 15, 433-459.

Güven, N. (1988) Smectites. In Hydrous phyllosilicates, Reviews in Mineralogy, Vol.19 (Bailey, S.W. Ed.). pp.725, Mineralogical Society of America, 497-559.

Hirowatari, F. and Katayama, N. (1973) Determination of the mineral compositions of the Toyoma slate and the Nachiguro shale by electron microanalysis. Science Report of Department of Geology, Kyushu University, 11, 311-319 (in Japanese with English abstract).

Kanisawa, S. and Ehiro, M. (1986) Occurrence and geochemical nature of phosphatic rocks and Mn-rich carbonate rocks in the Toyoman Series, Kitakami Mountains, Northeastern Japan. Journal of the Japanese Association of Mineralogists, Petrologists and Economic Geologists, 81, 12-31.

Kitano, Y. (1990) Geochemistry of carbonate deposits. pp.391, Tokai University Press. (in Japanese)

Matsunaga, K. (2000) The behavior of sulfur, phosphorus and carbon during the early stage of diagenesis : Isotope geochemistry of the Toyoman phosphatic rocks. pp.89, Master thesis of Shinshu University (MS). (in Japanese with English abstract)

Morikiyo, T. and Matsunaga, K. (2001) Origin of phosphatic rocks and carbonate rocks in the Toyoma Formation, Northeastern Japan : Pore water evolution during the early stage of diagenesis. Extended abstracts of 11th Annual V.M. Goldschmidt Conference, # 3066.

Open University Course Team (1989) Ocean Chemistry and Deep-Sea Sediments. pp.192, Butterworth-Heinemann, Oxford.

Swindale, L.D. and Fan, P.F. (1967) Transformation of gibbsite to chlorite in ocean bottom sediments. Science, 157, 799-800.